Observations of Coupled Spheroidal and Toroidal Modes

GUY MASTERS, JEFFREY PARK AND FREEMAN GILBERT

Institute of Geophysics and Planetary Physics, Scripps Institution of Oceanography, University of California, San Diego

In low-frequency seismic spectra the Coriolis force theoretically causes quasi-degenerate coupling of spheroidal and toroidal modes whose spherical harmonic degrees differ by unity and whose frequencies are close. It has been found that the coupling causes clearly observable effects on seismic spectra below 3.0 mHz. Many fundamental toroidal modes have a spheroidal component and vice versa. For example, the $_0S_l$ modes for $l = 8–22$ are significantly coupled to the $_0T_l$ modes for $l = 9–23$. The mean frequencies of pairs of coupled multiplets are repelled, and the mean attenuations are averaged. The shifting of complex frequencies must be adequately encompassed in the construction of spherically averaged and aspherical models of the density and elastic and anelastic structure of the earth. The coupling also causes variations in multiplet amplitudes which result in spectral peaks at toroidal mode frequencies on vertical and radial components and at spheroidal mode frequencies on transverse components. The variations must be taken into account in constructing Green's functions for the study of low-frequency source mechanisms.

1. INTRODUCTION

Splitting in low-frequency spectra was first observed in the analyses of the recordings of the great Chilean earthquake of May 22, 1960 [*Ness et al.*, 1961; *Benioff et al.*, 1961]. It was readily apparent that the observed splitting was caused primarily by the rotation of the earth [*Backus and Gilbert*, 1961; *MacDonald and Ness*, 1961; *Pekeris et al.*, 1961]. Coupling among multiplets was first treated theoretically by *Dahlen* [1969], and the effects of attenuation in coupling were shown by *Woodhouse* [1980]. As the calculations and observations reported here show, the importance of coupling is much more pervasive then previously realized.

Measurements of frequencies and attenuation rates of free oscillation multiplets are usually interpreted in terms of a spherically averaged earth structure. This procedure can be justified if the multiplets are isolated and departures of the real earth from the spherically averaged earth are small [*Gilbert*, 1971]. In this paper we show that for a more realistic model of the earth, one that is rotating and has small aspherical perturbations in structure, the assumption that a multiplet is isolated is often wrong and significant coupling of multiplets occurs over a large part of the spectrum. The consequences of the coupling are twofold: (1) elastic and anelastic spherically averaged models of the earth are biased unless the coupling effects are included, and (2) source mechanism retrieval from low-frequency data is biased unless coupling effects are included in the computation of the Green's functions.

The conclusions of this paper would be merely academic if the effects of coupling were not obvious in low-frequency data. The dominant signals in low-frequency seismograms are the fundamental spheroidal and toroidal mode multiplets. These multiplets are coupled together over a large frequency band, mainly by the Coriolis force, leading to very obvious effects in the data. It is clear, from the examples we give, that our ability to resolve earth structure and source mechanisms at low frequencies

will be limited by our ability to model the coupling effects.

Techniques for handling the computational problems associated with mode coupling are discussed in the next section. A more complete discussion will be given elsewhere (J. Park et al., manuscript in preparation, 1983). A comparison is made between computed coupling effects and observed effects in IDA (International Deployment of Accelerometers) data and GDSN (Global Digital Seismic Network) data. The computation is done via a Galerkin matrix method and includes rotation, ellipticity of figure, and attenuation. In some cases, nonaxisymmetric aspherical structure is included. The overall agreement between the computations and the observations is generally good but reveals the desirability of better spherically averaged and aspherical earth structures for modeling low-frequency seismograms.

2. RÉSUMÉ OF THE COMPUTATIONAL PROCEDURE

The Galerkin procedure that we have applied is closely related to the variational method for mode coupling described by *Luh* [1973]. In fact, in the absence of attenuation the equations are self-adjoint, and the Galerkin problem exactly coincides with the variational problem. Luh's formulation, in turn, derives from the correspondence between variational methods and first-order perturbation theory [*Moiseiwitsch*, 1966]. First-order perturbation theory based on Rayleigh's principle has been developed by *Dahlen* [1968, 1969], *Madariaga* [1971], *Zharkov and Lubimov* [1970a,b], *Woodhouse* [1976], and others. The relevant formulae are refined and summarized by *Woodhouse and Dahlen* [1978].

First-order perturbation theory has been used to calculate the splitting of isolated multiplets and the coupling between singlets of degenerate multiplets. Variational methods have been proposed to describe coupling without attenuation over many different multiplets [*Luh*, 1973; *Morris and Geller*, 1982; *Kawakatsu and Geller*, 1981]. However, calculations reported by *Woodhouse* [1980] indicate that attenuation significantly alters coupling between strongly coupled multiplets with different intrinsic attenuation rates. To include attenuation, the self-adjoint variational methods must yield to more general Galerkin pro-

cedures. The bonus of a more general procedure is that we can predict perturbations in apparent multiplet attenuation rates for comparison with measurements of average attenuation.

In the Galerkin procedure [*Kantorovich and Krylov*, 1958; *Mikhlin*, 1964; *Finlayson*, 1972; *Marchuk*, 1975; *Baker*, 1977] for an integrodifferential, linear operator, H, one chooses a sequence of basis functions $\{\phi_1, \phi_2, \cdots\}$ that satisfy the appropriate boundary conditions, possess the degree of smoothness required by H and that can be extended to a complete set. Any finite subset of the sequence must be linearly independent.

A solution to the eigenvalue problem

$$H\phi = \lambda\phi \qquad (1)$$

can be approximated within the subspace spanned by $\{\phi_1, \phi_2, \cdots, \phi_n\}$ by calculating the interaction among the basis vectors through the operator H. In this way (1) is converted into the $n \times n$ algebraic eigenvalue problem

$$Vx = \lambda Tx \qquad (2)$$

where

$$V_{ij} = (\phi_i^*, H\phi_j), \quad T_{ij} = (\phi_i^* \, \phi_j) \qquad (3)$$

and (,) denotes an inner product, usually an integration over the volume in which H is defined, with ϕ^* being the complex conjugate of ϕ.

We take as our basis set the elastic-gravitational eigenfunctions of a spherically symmetric earth model, usually the monopole of H. (At very low frequencies we include in our basis set the inner core toroidal modes, the outer core toroidal and gravitational elastic modes, and the secular modes, (iii)−(vi), described by *Dahlen and Sailor* [1979, p. 615]. This is done to ensure completeness.) The eigenfunctions are vector fields defined within the earth volume V and the associated all-space gravitational potentials. The vector fields are denoted $_n s_{\ell m}^q$, where n is the radial overtone number, ℓ is the degree (total angular order) of the spherical harmonic, m is the azimuthal order, and q is (S, T) for a (spheroidal, toroidal) mode.

The operator H can be written as

$$H = H_0 + H_1 \qquad (4)$$

where H_0 is the spherical average of H (the monopole) and H_1 represents rotation, ellipticity of figure, attenuation, and aspherical structure. The basis set is normalized

$$(_n s_{\ell m}^{q*}, _{n'} s_{\ell' m'}^{q'}) = \int_V dV \, \rho_0(r) \, _n s_{\ell m}^{q*} \cdot _{n'} s_{\ell' m'}^{q'}$$

$$= \delta_{nn'} \, \delta_{\ell \ell'} \, \delta_{mm'} \, \delta_{qq'} \qquad (5)$$

where $\rho_0(r)$ is the density for H_0 as a function of radius r. With the chosen normalization

$$(_n s_{\ell m}^{q*}, H_0 \, _{n'} s_{\ell' m'}^{q'}) = (_n \omega_\ell^q)^2 \, \delta_{nn'} \, \delta_{\ell \ell'} \, \delta_{mm'} \, \delta_{qq'} \qquad (6)$$

where $_n \omega_\ell^q$ is the degenerate eigenfrequency of the multiplet (n, ℓ, q). When $\|H_1\| \ll \|H_0\|$, V in (2) and (3) will be diagonally dominant.

We have used the formulae of *Woodhouse* [1980] to calculate the interaction due to rotation, ellipticity of figure, attenuation, and, in some cases, aspherical structure. For

any two eigenfunctions s_i, s_j of H_0

$$(s_i^*, H_1 s_j) = V_{ij} - \omega W_{ij} - \omega^2 T_{ij} \qquad (7)$$

where ω represents the eigenfrequency to be determined. In (7) we have suppressed any effects of physical dispersion [*Akopyan et al.*, 1975, 1976; *Liu et al.*, 1976; *Kanamori and Anderson*, 1977]. Including physical dispersion is important for interactions over a large frequency band, but for most interactions over small frequency bands, the center of the band can be taken as the reference frequency and physical dispersion can safely be neglected (J. Park et al., manuscript in preparation, 1983). The T_{ij} terms in (7) are properly placed in the kinetic energy matrix T in (2), which is Hermitian but not necessarily diagonal. The Coriolis force leads to the matrix W_{ij} in (7) and formally requires the solution of the quadratic eigenvalue problem

$$(V - \omega W - \omega^2 T)x = 0 \qquad (8)$$

By defining a vector $y = \omega x$, the quadratic problem (8) can be converted to a linear algebraic eigenvalue problem [*Garbow et al.*, 1977, pp. 49–50]

$$\begin{bmatrix} -W & V \\ I & O \end{bmatrix} \begin{bmatrix} y \\ x \end{bmatrix} = \omega \begin{bmatrix} T & O \\ O & I \end{bmatrix} \begin{bmatrix} y \\ x \end{bmatrix} \qquad (9)$$

at the expense of doubling its size. At frequencies below about 0.5 mHz, modes with relatively very different frequencies couple strongly, and the form (9) must be used. Such strong coupling is found to exist for $_1 S_1$, $_0 S_2$ and the Chandler wobble (primarily $_0 T_1$ in shape) [*Smith and Dahlen*, 1981], for example. However, in the present paper the observations of interest lie above 1 mHz, and the dominant coupling is confined to frequency differences about the same order of magnitude as the rotation rate (11.606 μHz). Thus we can apply (8) to narrow frequency bands. We have found that we can evaluate (7) in narrow frequency bands by approximating the term linear in ω

$$(s_i^*, H_1 s_j) = V_{ij} - U_{ij} - \omega^2 T_{ij} \qquad (10)$$

where

$$U_{ij} = (\omega_i \omega_j)^{1/2} W_{ij} \qquad (11)$$

This approximation does not significantly effect the numerical results for frequencies above 0.5 mHz.

With the indicated approximations the Galerkin procedure in narrow frequency bands is reduced to the general algebraic eigenvalue problem

$$(V - \omega^2 T)x = 0 \qquad (12)$$

where T is Hermitian positive definite and V, because of attenuation, is complex but not Hermitian. The system (12) is solved numerically with slight modifications of EISPACK routines (*Smith et al.* [1976] and see *Garbow et al.* [1977, pp. 49–50] for higher degree eigenvalue problems, e.g., (8)−(9)).

In this paper we are primarily concerned with coupling among fundamental spheroidal, $_0 S_\ell$, and toroidal, $_0 T_\ell$, modes. Coupling among fundamentals and overtones is small and has been neglected in the frequency band

1–5 mHz. Some overtones, e.g. $_7S_1$ and $_2T_2$, are strongly coupled but are not discussed here. Angular selection rules for coupling by rotation and ellipticity are simple. A mode $_nS_\ell$ can couple directly to $_{n'}T_{\ell\pm1}$, $_{n'}S_\ell$, $_{n'}S_{\ell\pm2}$. A mode $_nT_\ell$ can couple directly to $_{n'}S_{\ell\pm1}$, $_{n'}T_\ell$, $_{n'}T_{\ell\pm2}$. Other, indirect couplings are possible [Smith, 1977]. Rotation and ellipticity do not couple different azimuthal degrees m. We have used this fact, when aspherical structure is not included, to order the matrices V and T in (12) into block diagonal form to give a distinct eigenproblem for each value of m. The eigenvectors x_m for each m represent the hybrid singlets appropriate to the coupled problem. In almost all cases we find that one modal type predominates in the amplitude of the coupled singlets. We use the notation $(_0St_\ell, _0Ts_\ell)$ to represent a coupled multiplet whose major contribution comes from a multiplet of type $(_0S_\ell, _0T_\ell)$ and whose minor contribution is from $(_0T_{\ell'}, _0S_{\ell'})$, where $\ell' \neq \ell$.

Our calculations show that Coriolis coupling is the dominant effect. Our approach, via an integral equation, can be applied to a greater band of frequencies than can the first-order perturbation approach [Luh, 1973, 1974]. Furthermore, the vital effect of attenuation is included in our calculations following the formulation of *Woodhouse* [1980].

To see why Coriolis coupling is dominant, we offer the following hueristic argument. Consider the W matrix in (7)–(9):

$$W_{12} = 4 \int_V \rho_0(r) \, [s_1 \cdot (i\Omega \times s_2)^* \, dV] \qquad (13)$$

where s_1, s_2 are any two eigenfunctions and Ω is the sidereal angular velocity vector. The vector cross product in (13) rotates $(_nS_\ell, _nT_\ell)$ motion into $(_nT_{\ell\pm1}, _nS_{\ell\pm1})$ motion quite efficiently. This leads to strong coupling in the 1.5 to 3.0-mHz frequency band where such modes are close in frequency. In contrast, coupling through ellipticity can be regarded as diffraction of spherical waves by the surface of the earth. The surficial wave number of most modes is large compared to that of the earth's equatorial bulge. In fact, the ratio of wave numbers for a mode of angular order ℓ is roughly $\ell/2$ (there is additional variation with azimuthal order). We therefore expect the diffraction of toroidal motion into spheroidal motion and vice versa to be small for ellipticity or any other very long wavelength lateral structure, such as the transition zone model of *Masters et al.* [1982]. Such diffraction is much less efficient than rotation as a coupling mechanism.

This hueristic argument is in agreement with the results reported by *Luh* [1974]. Using quasi-degenerate perturbation theory, he computed the effect of rotation, ellipticity of figure, and the continent-ocean aspherical structure on multiplets very close in frequency. He found that Coriolis coupling between a spheroidal and a toroidal multiplet overshadows all other types of coupling. This means that at the frequencies considered in this report, aspherical structure, including any of the tectonically regionalized structures [e.g., *Silver and Jordan*, 1981], is not as important as the Coriolis force in coupling multiplets. At higher frequencies, above 3.0 mHz say, the effect of aspherical structure will become more important, and rotation can eventually be neglected.

In order to compare our coupling calculations with data, we calculate the mean singlet frequency of the hybrid multiplets $_0St_\ell$. The grouping of hybrid singlets into distinct hybrid multiplets remains well defined even for profoundly coupled modes like $_0S_{11}-_0T_{12}$. Only when the coupled multiplets are very nearly degenerate in both frequency and attenuation does the distinct grouping disappear. We determine the average attenuation of the hybrid multiplet $_0St_\ell$ by averaging over the imaginary part of the singlet eigenfrequencies.

We can gain insight into the qualitative features of strong coupling with a simplified example. Consider coupling between zeroth-order singlets $_0S_\ell^m$ and $_0T_{\ell+1}^m$. If we consider only attenuation and coupling due to Coriolis force, the potential energy coupling matrix takes the form

$$V = \begin{bmatrix} (\omega_S)^2 & \epsilon \\ \epsilon & (\omega_T)^2 \end{bmatrix} \qquad (14)$$

where ω_S, ω_T are the (complex) spheroidal and toroidal singlet eigenfrequencies and ϵ is the coupling between $_0S_\ell^m$ and $_0T_{\ell+1}^m$ due to Coriolis force. The hybrid eigenfrequencies are defined by

$$\omega_\pm^2 = \frac{\omega_S^2 + \omega_T^2}{2} \pm \frac{1}{2}((\omega_S^2 - \omega_T^2)^2 + 4|\epsilon|^2)^{1/2} \qquad (15)$$

Since $\text{Re}[(\omega_S^2 - \omega_T^2)^2 + 4|\epsilon|^2]^{1/2} \geq \text{Re}(\omega_S^2 - \omega_T^2)$, the hybrid eigenfrequencies repel, as is well known from examples in mechanics [*Sommerfeld*, 1952, pp. 106–111]. Since $|\text{Im}[(\omega_S^2 - \omega_T^2)^2 + 4|\epsilon|^2]^{1/2}| \leq |\text{Im}(\omega_S^2 - \omega_T^2)|$, the hybrid attenuations will attract. One expects that strong coupling would tend to homogenize singlet attenuation rates. If we assume that $\text{Re}(\omega_S) > \text{Re}(\omega_T)$, define $\tau = \omega_+ - \omega_S$ and $\Delta\omega = \omega_S - \omega_T$, we can express (15) as

$$\left[\tau + \frac{\Delta\omega}{2}\right]^2 = \frac{|\epsilon|^2}{4\omega_S^2} + \frac{(\Delta\omega)^2}{4} + O\left[\frac{(\Delta\omega)^3}{\omega_S}\right] \qquad (16)$$

We can express $|\epsilon|^2$ [*Dahlen*, 1969, equation 23]:

$$|\epsilon|^2 = 4\omega_+^2 \Omega^2 a^2 \left[\frac{\ell^2 - m^2}{4\ell^2 - 1}\right] \qquad (17)$$

where Ω is the rotation frequency and a is a dimensionless scalar near unity. We can take ω_S for ω_+ in (17) without changing terms of highest order and average (17) over all azimuthal orders $|m| \leq \ell$ to obtain

$$\langle \epsilon^2 \rangle_m = \frac{2}{3} \omega_S^2 \Omega^2 a^2 \frac{\ell}{\ell + \frac{1}{2}} \qquad (18)$$

where $\langle \ \rangle_m$ denotes expectation value over m. We specify $\Delta\omega$ to be constant over m. This is not generally true, but is a useful approximation. Solving (16) for $|\tau|$ and using (18) in place of $|\epsilon|^2$ gives the approximate result:

$$|\tau| \approx \frac{1}{2}\left[\left[\frac{2}{3}\Omega^2 a^2 \frac{\ell}{(\ell + \frac{1}{2})} + (\Delta\omega)^2\right]^{1/2} - \Delta\omega\right] \qquad (19)$$

If $\text{Re}(\omega_T) > \text{Re}(\omega_S)$, the sign of τ will be negative. Equation (19) shows how mean frequency shifts become appreciable whenever the frequency difference between coupled modes is of the same order as, or smaller than,
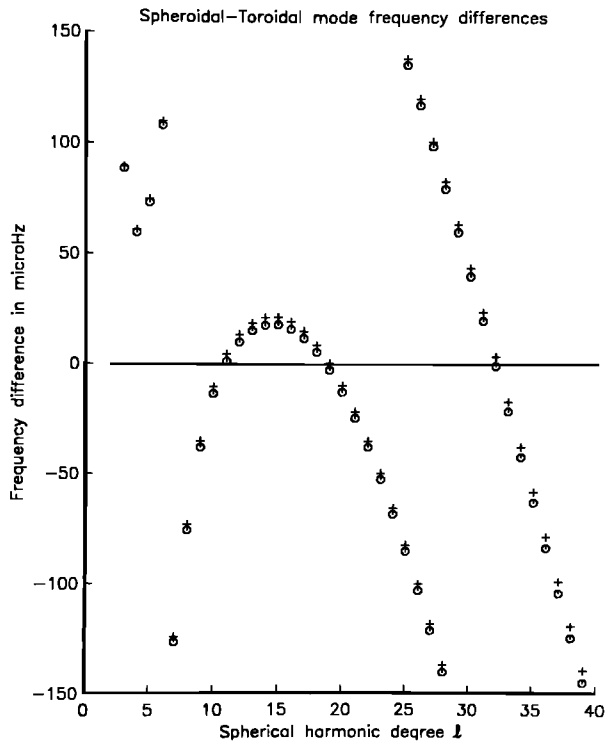
Spheroidal—Toroidal mode frequency differences

Fig. 1. Frequency differences, in μHz, between fundamental $_0S_\ell$ and $_0T_{\ell+1}$ modes for $\ell = 7-28$ and between fundamental $_0S_\ell$ and $_0T_{\ell-1}$ modes for $\ell = 3-6$ and $\ell = 25-39$. The plus sign denotes values for the anisotropic PREM model [*Dziewonski and Anderson*, 1981], and the dot for model 1066A [*Gilbert and Dziewonski*, 1975].

the earth rotation frequency (11.606 μHz). The frequency differences between neighboring $_0S_\ell$ and $_0T_{\ell\pm1}$ modes are shown in Figure 1. The toroidal and spheroidal frequencies, as functions of ℓ, cross near $_0S_{11}$, $_0S_{19}$, and $_0S_{32}$. The

features in Figure 1 vary little for many modern earth models and imply strong Coriolis coupling for $\ell = 10-20$ and near $\ell = 32$.

3. COMPUTATION AND OBSERVATION OF FREQUENCY SHIFTS AND AMPLITUDE VARIATIONS

The calculations of the preceding section predict several features that can be seen in low-frequency data. The interaction is such that unless the coupled $_0S_\ell$ and $_0T_{\ell\pm1}$ modes are nearly degenerate in their frequencies, singlets are grouped together in hybrid multiplets which have predominantly toroidal (Ts) or spheroidal (St) characteristics. In the case of near-degeneracy, i.e., when the singlets of coupling multiplets are overlapped in complex frequency, the separation into hybrid multiplets is not always clear, and the coupled multiplets (a super multiplet) must be considered as a single entity. Most earth models predict near-degeneracy for the multiplets $_0S_{11}-_0T_{12}$, $_0S_{19}-_0T_{20}$, and $_0S_{32}-_0T_{31}$, as shown in Figure 1. We shall demonstrate that the first two are well observed but that the latter is by no means obvious in the data.

The model we have chosen for demonstrating the coupling effects is model 1066A of *Gilbert and Dziewonski* [1975]. This is an isotropic model and provides the best fit to the existing mode dataset for frequencies below about 5 mHz. The model is not optimal in that it was constructed without consideration of the effects of physical dispersion and furthermore does not fit the fundamental spheroidal mode data well above angular order 30. A new model is highly desirable but will have to await a more complete evaluation of bias in the mode dataset.

To illustrate the coupling behavior, we show computed results for the multiplet pair $_0S_{14}-_0T_{15}$. In model 1066A, $\Delta\omega/2\pi \simeq 18\ \mu$Hz for this pair. In Figure 2a, we plot singlet eigenfrequencies versus $1000/Q$ for two cases: (1)
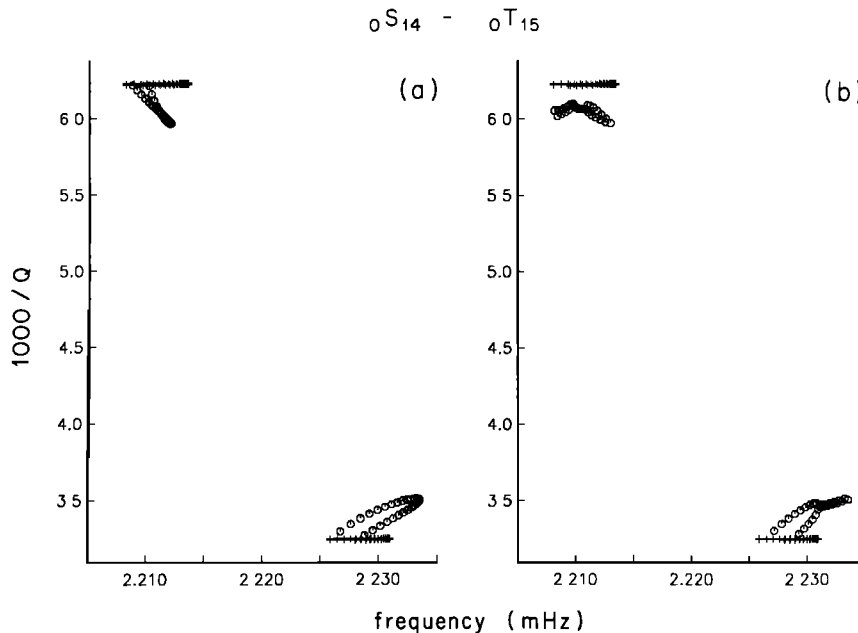

Fig. 2. Coupling between $_0S_{14}$ and $_0T_{15}$. (a) No coupling (plus signs) versus coupling (octagons) among all nearby (±1 mHz) fundamental modes due to rotation, ellipticity and attenuation. (b) No coupling (plus signs) versus coupling (octagons) between $_0S_{14}$ and $_0T_{15}$ due to rotation, ellipticity, attenuation, and aspherical structure of *Masters et al.* [1982].
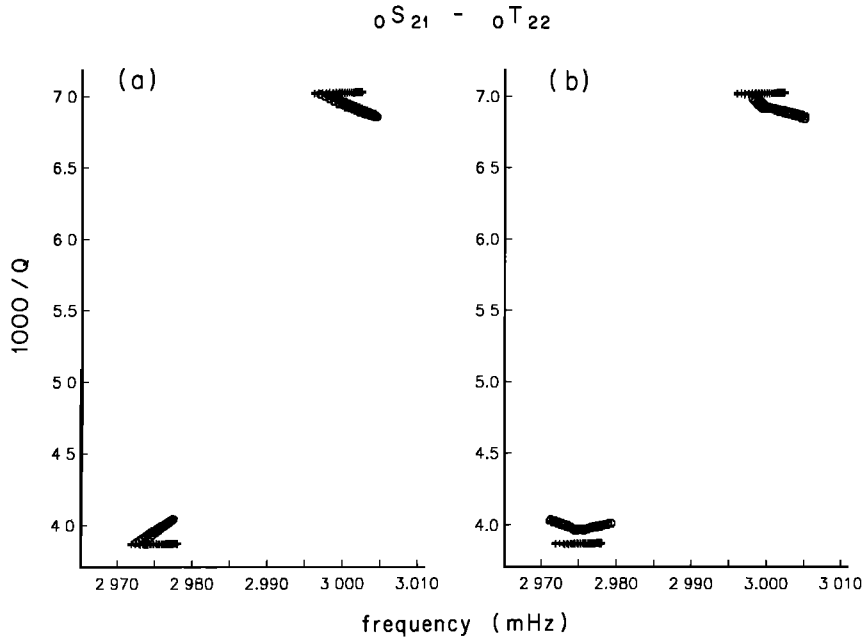
$_0S_{21}$ - $_0T_{22}$

Fig. 3. Coupling between $_0S_{21}$ and $_0T_{22}$. Details as in Figure 2.

no coupling between the two multiplets, and (2) unrestricted coupling, due to rotation, ellipticity, and attenuation, among the fundamental modes $_0S_7-_0S_{23}$ and $_0T_7-_0T_{24}$ (all within ± 1 mHz of $_0S_{14}-_0T_{15}$). Only the singlets of $_0S_{14}$ and $_0T_{15}$ enter strongly in the coupling of that pair of multiplets. Figure 2a is imperceptibly different if the basis $_0S_{14}-_0T_{15}$ is used in place of the larger one. In Figure 2b we compare the uncoupled case to coupling due to rotation, ellipticity, attenuation, and the $\ell = 2$ transition zone anomaly inferred by Masters et al. [1982] in their study of fundamental mode peak shifts. Only $_0S_{14}$ and $_0T_{15}$ are included in the calculations for Figure 2b. The transition zone model breaks azimuthal symmetry, causing more general coupling and increasing the effort required to

solve the matrix eigenvalue problem. Azimuthal symmetry breaking is caused by any aspherical structure that is not rotationally symmetric, e.g., any of the popular, tectonically regionalized models. We have chosen the transition zone model simply to illustrate the effect of aspherical structure. In fact, once we can successfully account for rotation and ellipticity of figure in the coupled multiplets, the remaining features must be caused by aspherical structure including, perhaps, anisotropy. It is the revelation of aspherical structure that is the ultimate goal of studying coupling and splitting.

The qualitative behavior for the more complicated model is similar to that of the model without the Masters et al. [1982] anomaly. The mean multiplet peak shifts are
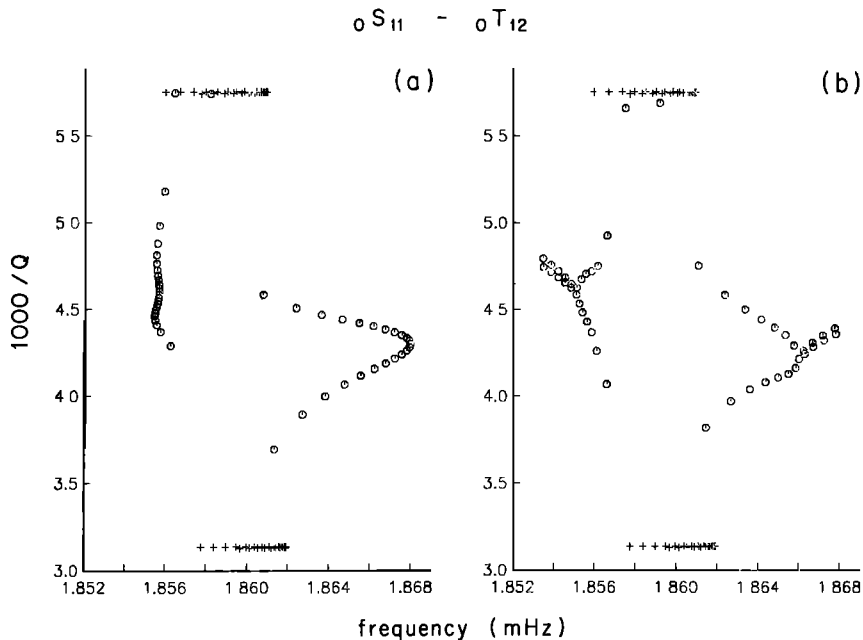
$_0S_{11}$ - $_0T_{12}$

Fig. 4. Coupling between $_0S_{11}$ and $_0T_{12}$. Details as in Figure 2.

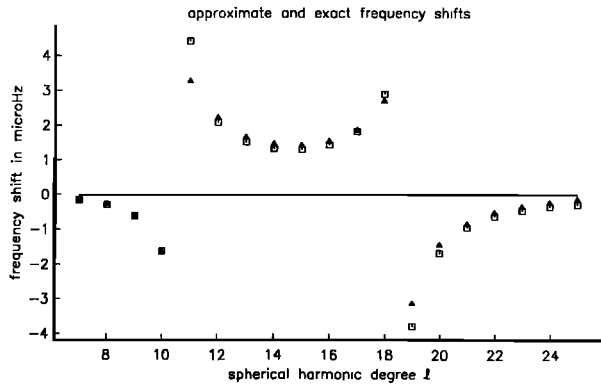Fig. 5.   Mean frequency shifts of $_0St_f$ hybrid multiplets relative to the unperturbed $_0S_f$ multiplets for model 1066A. The effects of rotation, ellipticity and attenuation have been computed. Triangles denote results of the full Galerkin calculation. Squares denote values derived from (19). The basis set used in the calculations consists of all fundamental modes below 6 mHz.

dominated by Coriolis coupling. A similar comparison holds true for Figure 3, where the frequencies of $_0S_{21}$ and $_0T_{22}$ are seen to couple weakly. The basis for Figure 3a is all fundamentals within ± 1 mHz of $_0S_{21}$ and $_0T_{22}$. In Figure 3b the basis is $_0S_{21}-_0T_{22}$. Coupling for $_0S_{11}$ and $_0T_{12}$ is shown in Figure 4. The basis for Figure 4a is all fundamentals within ± 1 mHz of $_0S_{11}-_0T_{12}$ and for Figure 4b is $_0S_{11}-_0T_{12}$. $_0S_{11}-_0T_{12}$ is well known as a strongly coupled multiplet pair, with many spheroidal and toroidal singlets interlaced in frequency. Figure 4a makes clear that the two types of zeroth-order singlets, however, are well separated in attenuation. $_0S_{11}$ and $_0T_{12}$ couple to form two distinct groups of singlets, aside from two relatively uncoupled toroidal singlets corresponding to $_0T_{12}$. These can be thought of as hybrid multiplets, quasi-toroidal $_0Ts_{12}$ and quasi-spheroidal $_0St_{11}$. The frequency shifting is much greater than in the earlier example and is strongly affected by the addition of the *Masters et al.* [1982] asphericity.

The overlap in singlet attenuation rates of the two hybrid multiplets is due to spheroidal-dominant singlets in the $_0Ts_{12}$ multiplet and toroidal-dominant singlets in the
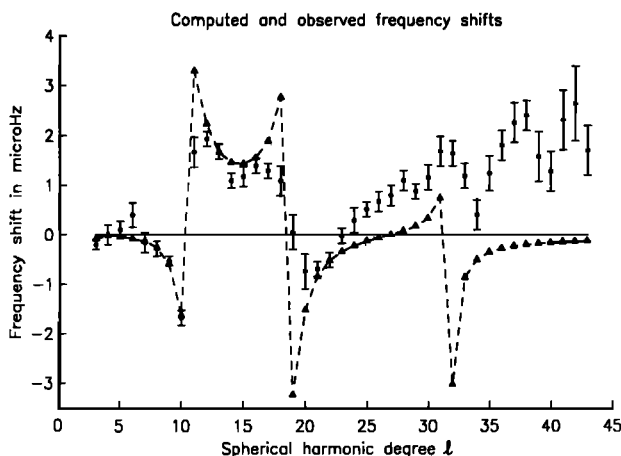
$_0St_{11}$ multiplet. This is due to reversals in the interlacing of the zeroth-order spheroidal and toroidal singlet real-part frequencies caused by the fact that the first-order rotational splitting of $_0S_{11}$ is opposite to that of $_0T_{12}$ (i.e., the Coriolis splitting parameter for $_0S_{11}$ is negative). Relative spacing of zeroth-order singlet eigenfrequencies is highly variable in closely spaced multiplet pairs, leading to a breakdown in the accuracy of (19). To demonstrate this, we show in Figure 5 mean frequency shifts of hybrid multiplets, $_0St_f$, relative to the degenerate eigenfrequency of the zeroth-order multiplets, $_0S_f$, for model 1066A. All calculations were done with rotation, ellipticity, and attenuation included. The $_0S_f$ and $_0T_{f+1}$ dispersion branches cross near $f = 11$ and $f = 19$, where we observe "tears" in the computed frequency shifts. Shifts calculated from (19) are plotted for $f < 25$ as a comparison. As expected, (19) fails near the "tears."

The results in Figure 5 show clearly the failure of the diagonal sum rule [*Gilbert*, 1971] when the conditions for its application are violated. In the presence of coupling, the generalization of *Woodhouse* [1980] must be used. In the present situation the mean frequency and attenuation of each super multiplet, $_0St_f + _0Ts_{f+1}$, $f = 8-22$, is required. Although there are very many observations of $_0St_f$ modes, there are very few observations of $_0Ts_f$ modes. Until such observations are available we cannot use the generalized diagonal sum rule.

We have demonstrated that the hybrid multiplets with dominantly spheroidal characteristics (St modes) have a mean frequency which is shifted from that of a pure spheroidal mode. This is illustrated in Figure 6 where observed St means [*Masters and Gilbert*, 1983] (see the appendix) and calculated St means, shown in Figure 5, are graphed relative to model 1066A. The deviation of the calculated St means from 1066A is a result of the
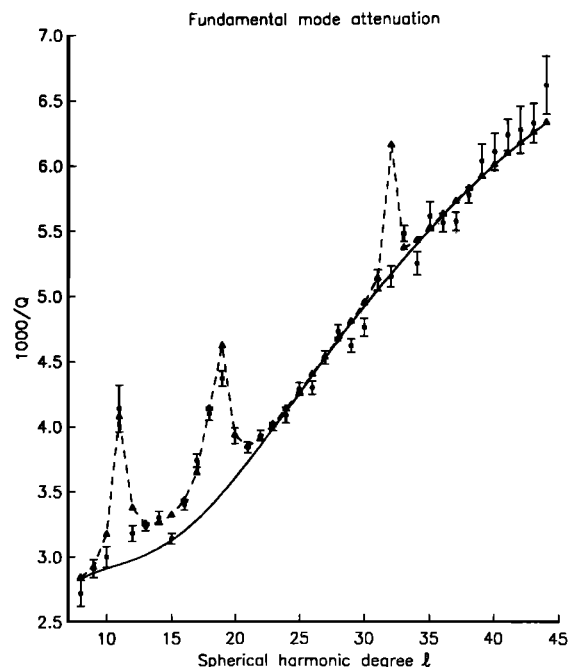

Fig. 6.   Observed mean frequencies (dots with error bars) and calculated mean frequencies (triangles) of $_0St_f$ hybrid multiplets relative to the unperturbed $_0S_f$ multiplets for model 1066A. The calculations are the same as those in Figure 5.

Fig. 7.   Observed attenuation (dots with error bars) and calculated attenuation (triangles) for $_0St_f$ modes and calculated attenuation (continuous curve) for $_0S_f$ modes for model 1066A. The calculations are the same as those in Figure 5.
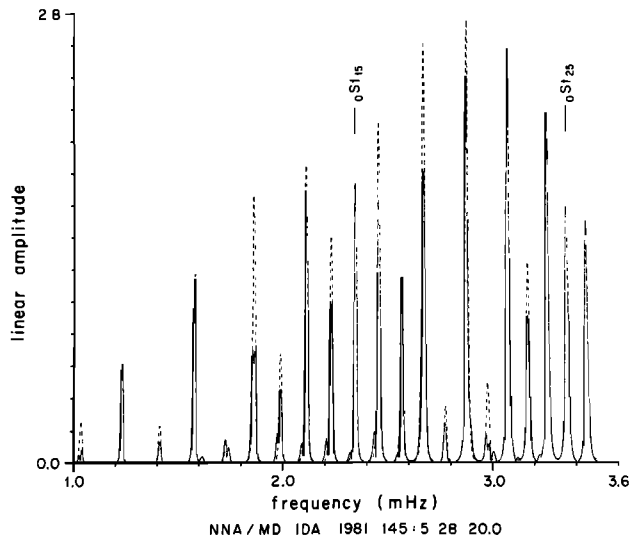
Fig. 8a. Amplitude spectra for fundamental modes on a vertically polarized accelerometer. Unperturbed spectrum (dashed line) versus the spectrum for modes coupled by rotation, ellipticity and attenuation (solid line). In the latter, coupling among all angular orders $\leqslant 26$ has been computed.
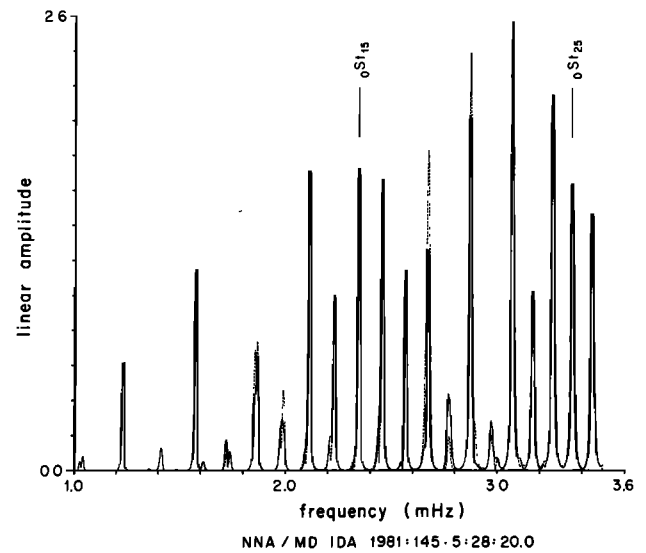

Fig. 8c. Comparison of coupling between nearest neighbors with (solid line) and without (dashed line as in Figure 8b) the aspherical structure of Masters et al. [1982].

spheroidal-toroidal multiplet coupling and frequency repulsion. Adding the aspherical structure of Masters et al. [1982] causes only very minor changes to the calculated St means. The coupling between $_0S_{11}$ and $_0T_{12}$, and $_0S_{19}$ and $_0T_{20}$, is so strong that our observed means are not just means of St modes but a mixture of Ts and St modes so the "tears" are not as pronounced as in the calculation. The St means for $_0S_{7-10}$, $_0S_{12-18}$ and $_0S_{20-25}$ are quite well predicted, though the model could clearly be improved.

Above $\ell = 26$ the model systematically underpredicts the frequencies, but more importantly, there is a predicted tear at $\ell = 32$ which is not present in the data. A preliminary investigation of transverse components obtained from the GDSN indicates that model 1066A systematically overpredicts the toroidal mode frequencies by about $6\ \mu$Hz at $\ell = 31$. The difference in frequency between

$_0T_{31}$ and $_0S_{32}$ for a spherically averaged earth should therefore be $6-7\ \mu$Hz rather than the 0.6 μHz given by 1066A. The additional separation in frequency is enough to remove the predicted strong coupling at the crossover of the toroidal and spheroidal branches.

Another feature of the St modes predicted by the calculation is the shifting of the mean Q^{-1} away from that of a pure spheroidal mode. This is illustrated in Figure 7. The Q model used in the calculation is taken from the appendix and predicts the spheroidal mode attenuation shown by the solid line. The calculated St mode attenuations are shown by the triangles, and below $\ell = 30$, their behavior is clearly reflected in the data. The predicted behavior at $\ell = 32$ is not seen in the data, again suggesting that the crossover of the toroidal mode and spheroidal mode branches is incorrectly predicted by the model.
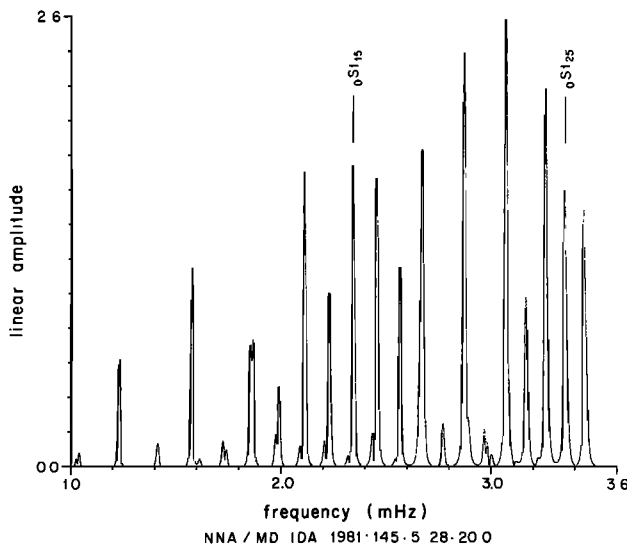
While constructing the Q model in their Table 9, Mas-

Fig. 8b. Comparison of coupling between nearest neighbors (dashed line) and all angular orders $\leqslant 26$ (solid line as in Figure 8a).
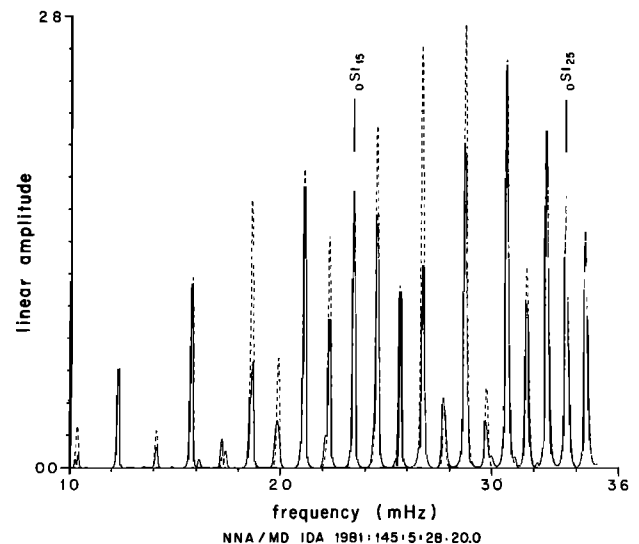

Fig. 8d. Comparison of coupling between nearest neighbors, including aspherical structure (solid line as in Figure 8c) and the unperturbed spectrum (dashed line as in Figure 8a).
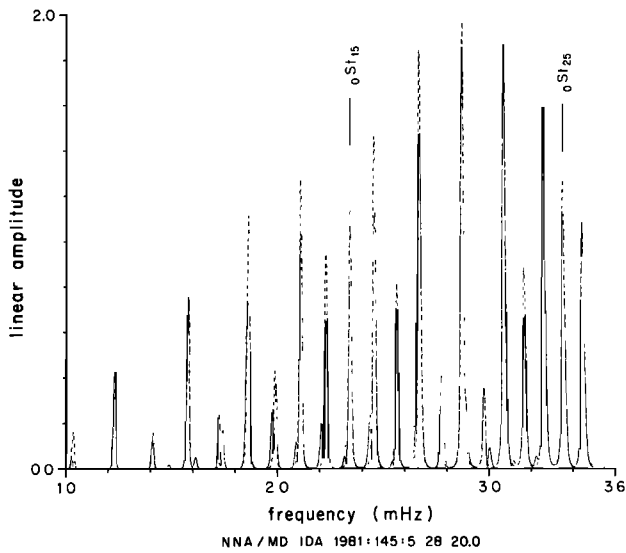
Fig. 9a. Comparison of coupled (solid line) and uncoupled (dashed line) amplitude spectra for a shallow, strike-slip source.

ters and Gilbert [1983] realized that the data for angular orders 11, 18, and 19 were biased by coupling effects and were not pure spheroidal mode attenuation measurements. They did not realize that all the measurements for $\ell = 10 - 21$ are significantly biased, and this led to a model with a lower mantle which is too highly attenuating. Further modeling of high-quality attenuation measurements must incorporate the coupling effects, and a preliminary result is presented in the appendix.

The same point is also true for the frequency data. The pattern of frequency shifts in Figure 6 was first noted by *Silver and Jordan* [1981] and is present in the data used to construct current earth models. These data obviously cannot be regarded as belonging to pure spheroidal modes, and their errors are now sufficiently small that a bias of 10 or more standard deviations could result if mode coupling effects were not considered.

In summary, we believe that these results demonstrate the importance of considering mode coupling when con-
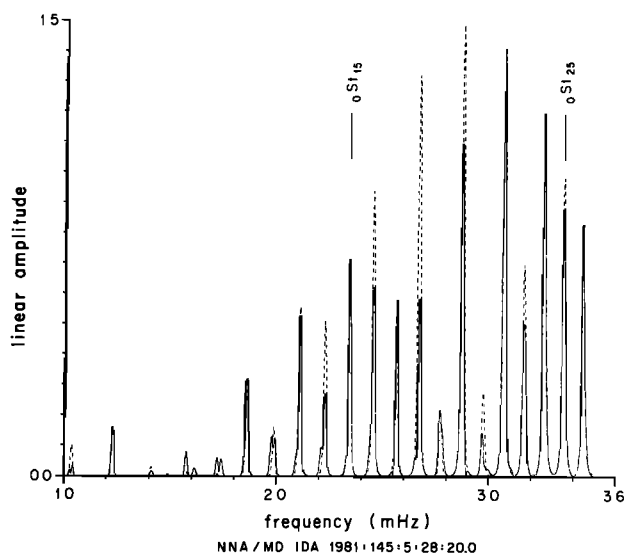
structing more accurate, spherically averaged earth models.

Another important consequence of our calculations is the predicted mode mixing. An example of this is the appearance, on the spectra of vertical component seismic data, of resonance peaks at frequencies appropriate to toroidal multiplets. As we have seen, the coupled quasi-toroidal multiplet $_0Ts_\ell$ contains components of spheroidal motion. These components cause the predicted resonance peak in the vertical component spectrum. The horizontal component seismic data, after rotation into radial and transverse components, will show similar, apparently anomalous peaks. A certain amount of spheroidal motion in the transverse component and toroidal motion in the radial component occurs independent of coupling effects, its amount varying as the inverse of mode angular order ℓ. For large ℓ this effect is small, and Coriolis coupling should be the stronger effect.

We first demonstrate the mode mixing effects with some synthetic examples. We have used a double couple point source located at 48.8°S, 164.4°E and have computed synthetic seismograms for various source depths, source mechanisms and coupling effects at the IDA station NNA. Only fundamental mode toroidal and spheroidal modes are included in the calculation. Figure 8 illustrates the results for a 10-km-deep thrust mechanism dipping at 45° and striking north. The spectra have been computed for a 40-hour record length which has been tapered using a Hanning window. Figure 8a is a comparison of a spectrum for no coupling with that of coupling due to the Coriolis force and ellipticity. Ts modes are clearly visible and, as expected, are located approximately at the toroidal mode degenerate frequencies. It should be noted that tapering is essential to reduce sideband leakage in the spectrum which otherwise masks the Ts modes. This fact might explain why Ts modes have not previously been

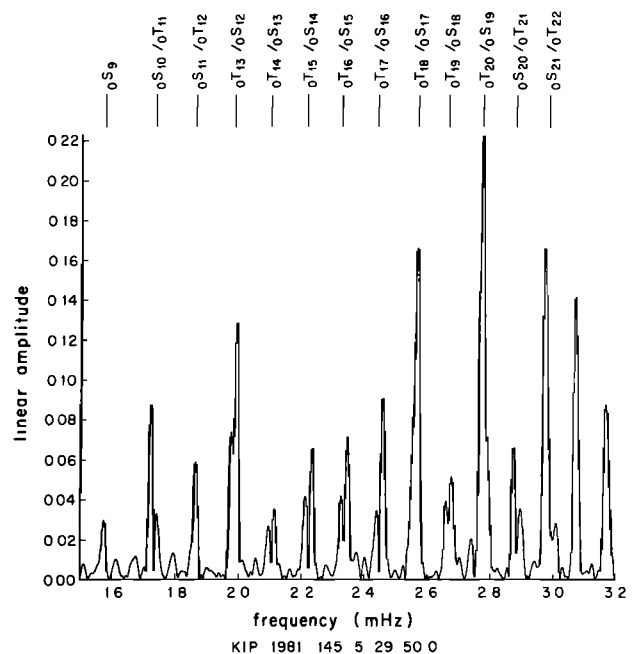Fig. 9b. As in Figure 9a for a deep, thrust source.

Fig. 10. Observed spectrum showing Ts modes on a vertically polarized IDA (La Coste-Romberg) accelerometer. A 35-hour record has been Hanning-tapered to produce the spectrum. The station/source for this spectrum is KIP/New Zealand 1981.

observed in real data. A long record length is also required to give the frequency resolution necessary to separate the *Ts* and *St* modes. It should be emphasized that this has the effect of suppressing the amplitude of the *Ts* modes relative to the *St* modes, as they generally have a higher attenuation rate. Deviations in the coupled spectrum from the uncoupled spectrum are quite pronounced throughout this frequency band (1.0–3.5 mHz).

This calculation is complete in that coupling between all singlets ($\ell \leq 26$) of the same azimuthal order has been included. If we restrict the calculation to coupling between nearest neighbor $_0S_\ell$, $_0T_{\ell+1}$ modes, we have the result in Figure 8b. This demonstrates that basically all the coupling in this frequency band is due to nearest neighbors.

An additional aspherical structure greatly increases the labor involved in solving the coupling problem so we demonstrate the effect by including only nearest neighbor $_0S_\ell$, $_0T_{\ell+1}$ modes. The $\ell = 2$ transition zone model of *Masters et al.* [1982] has been employed, and the result is shown in Figure 8c. The spectrum including coupling effects due to rotation, ellipticity, and aspherical structure is compared with the spectrum including coupling effects due to ellipticity and rotation between nearest neighbors. The two spectra are very similar except that there appears to be some broadening of the hybrid multiplets due to the aspherical structure. This effect makes the *Ts* modes less clear when compared with the uncoupled spectrum as illustrated in Figure 8d.

We think that these calculations show that the dominant coupling effect in this frequency band is the Coriolis force acting on nearest neighbor $_0S_\ell$, $_0T_{\ell+1}$ modes. The amplitude differences between coupled and uncoupled multiplets are similar to those observed between real data and synthetics computed using a spherically symmetric earth model [*Riedesel et al.*, 1981] and certainly cannot be regarded as small. Large-scale coupling experiments have been made in which Coriolis coupling between spheroidal

Fig. 11. As in Figure 10 for the UCLA (La Coste-Romberg) station (South Pole)/source: SPA/New Zealand 1981.
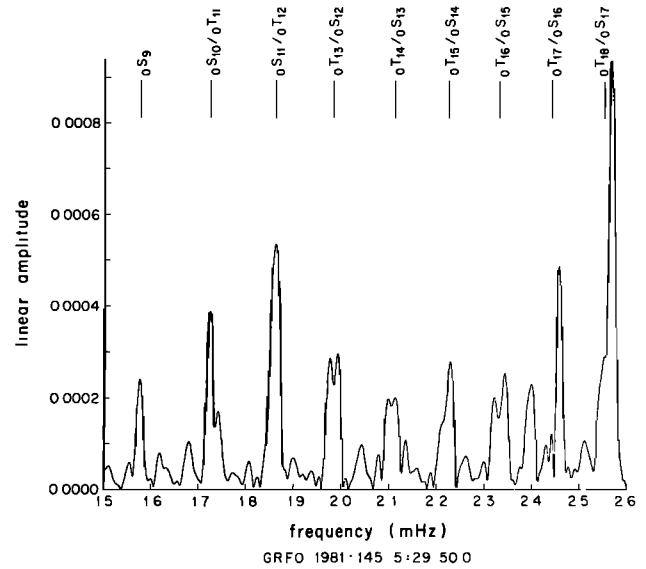
Fig. 12. As in Figure 10 for a vertically polarized SRO accelerometer: GRFO/New Zealand 1981.

and toroidal modes was not included (J. H. Woodhouse, personal communication, 1982). The amplitude variations in these restricted calculations did not exceed 10%.

We have investigated the effect of varying the source parameters and illustrate some of the results in Figure 9. Figure 9a shows the effect of a strike-slip source located at 10-km depth with a northerly strike and a vertical fault plane. The toroidal modes are better excited relative to the spheroidal modes for this kind of source; consequently, the *Ts* modes are more pronounced. The coupling calculation includes the effects due to rotation and ellipticity. The differences between the coupled and uncoupled spectra are again quite pronounced over the whole frequency interval.

Figure 9b gives a comparison for a deep thrust event located at 600-km depth. The coupling calculation includes only the effects due to rotation and ellipticity. We had expected the differences between the coupled and uncoupled spectra to be less for deep earthquakes as the toroidal excitations are very small. This is not the case, and the coupling again gives *Ts* modes and strong variations in the amplitudes of the *St* modes.

If we inspect vertical component spectra of earthquakes which are rich in low-frequency toroidal mode energy, the synthetic calculations suggest that the *Ts* modes should be clearly visible. The station geometry used in these examples is that of an event which occurred on May 25, 1981. Data from this event have provided the clearest observations of *Ts* modes to date. Figures 10–13 give examples from different kinds of vertical component instruments recording this event. All spectra are for 35-hour time intervals and have been tapered using the Hanning window. *Ts* modes are clearly visible at nearly all stations and are easily identified on IDA and GDSN instruments. It is easy to show that *Ts* modes behave like quasi-toroidal modes with a higher attenuation rate than the *St* modes by computing spectra for different start times. As the start time is delayed relative to the origin time of the event, the *Ts* modes decay relative to the *St* modes (Figure 14). We
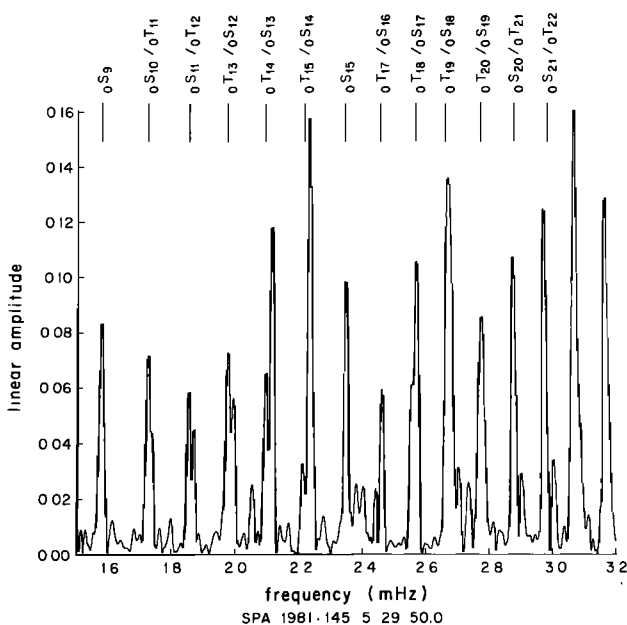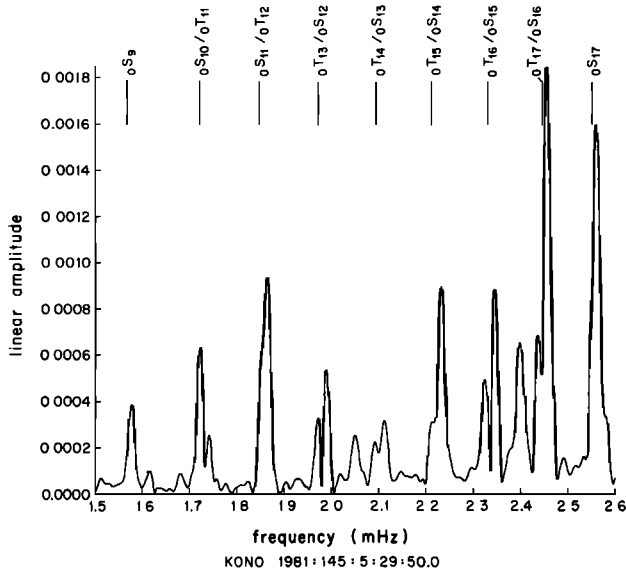
Fig. 13. As in Figure 10 for a vertically polarized ASRO accelerometer: KONO/New Zealand 1981.

again emphasize that the procedures we have used to enhance frequency resolution in the spectra (long record length and tapering) suppress the apparent amplitudes of the Ts modes relative to the St modes because of the difference in attenuation rate. In some of the examples (e.g., KIP) the initial amplitudes of the Ts modes are comparable with the initial amplitudes of the St modes. It is clear that unless we model the coupling effects we will not be able to perform detailed modeling of the source in this frequency band.

These observations establish Ts modes as a reality and suggest a solution for another observational problem we have encountered when one rotates horizontal component seismograms to get a transverse and a radial component. On a true (transverse, radial) component without coupling the $(_nS_l, _nT_l)$ modes should be reduced approximately a factor of l relative to the other component. Thus both components should show both mode types for low l but not for $l \gg 1$. In Figure 15 we have the spectrum of the radial component of NWAO/Tonga 1977. With the exception of the low l, $_1T_2$ mode all modes are $_nS_l$ modes. There are no $_0T_l$ modes except the strongly coupled $_0T_{12}-_0S_{11}$ pair. Also in Figure 15 is the spectrum of the transverse component of NWAO/Tonga 1977. Below 1.7 mHz the only $_nS_l$ mode is $_2S_6$, strongly excited on the radial component and down a factor of 3.4 here, and there are no $_0S_l$ modes. We think that these results mean that the instruments are properly calibrated. However, above 1.7 mHz there are several examples of $_0S_l-_0T_{l+1}$ coupling. This pattern is repeated for ANMO/Tonga 1977 whose radial and transverse spectra are shown in Figure 16. Again, below 1.7 mHz the radial spectrum is dominantly $_nS_l$ and the transverse spectrum is dominantly $_nT_l$, implying good calibration. Again, above 1.7 mHz there is evidence of $_0S_l-_0T_{l+1}$ coupling with some prominent St modes on the transverse component. This is a common feature of spectra from 1.7 to 2.7 mHz on rotated components of both SRO and ASRO horizontals. The Tonga event did not excite toroidal modes as strongly as

spheroidal modes so Ts modes are weak on both the vertical and radial components. Conversely, the St modes are relatively strong on the transverse component. As most large events are of thrust or normal type, like the Tonga event, it may be difficult to get measurements of Ts modes from transverse components because of the proximity of the strong St modes.

4. DISCUSSION

At frequencies below 3.0 mHz, fundamental spheroidal and toroidal modes are coupled strongly and are observed as hybrid multiplets which are shifted in both mean frequency and attenuation rate from the uncoupled values. Except for very strong coupling, the hybrid multiplets are predominantly spheroidal (St modes) or toroidal (Ts modes) in character. We have demonstrated that the shifts in the mean frequencies and attenuation rates of St modes can be predicted by considering the coupling effects of rotation, attenuation, and ellipticity of figure. Of these, the first is dominant and the second is very important. We have not found it necessary to include anisotropy in the calculations. If anisotropy is confined to the upper mantle, then coupling effects may become noticeable at frequencies higher than 3.0 mHz as the energy distribution of the modes becomes more concentrated in this region. (It should also be remembered that a transversely isotropic model, such as PREM, would not give any coupling. Coupling occurs only when spherical symmetry is broken.) Another factor which argues strongly for the dominance of Coriolis coupling is that the coupling appears to be confined to nearest neighbors in the data, i.e., $_0S_l-_0T_{l+1}$
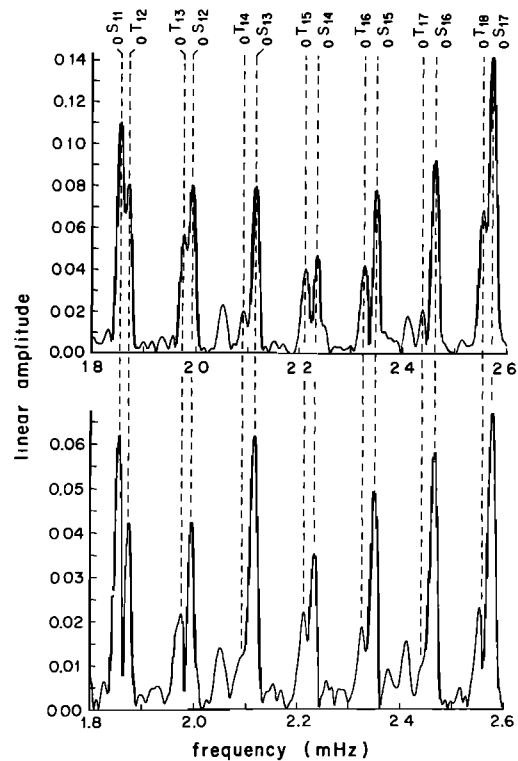

Fig. 14. As in Figure 10 for CMO/New Zealand 1981. The upper spectrum corresponds to a start time of 0 hours, and the lower 5 hours. The time lapse spectra show that Ts modes attenuate more rapidly than St modes.
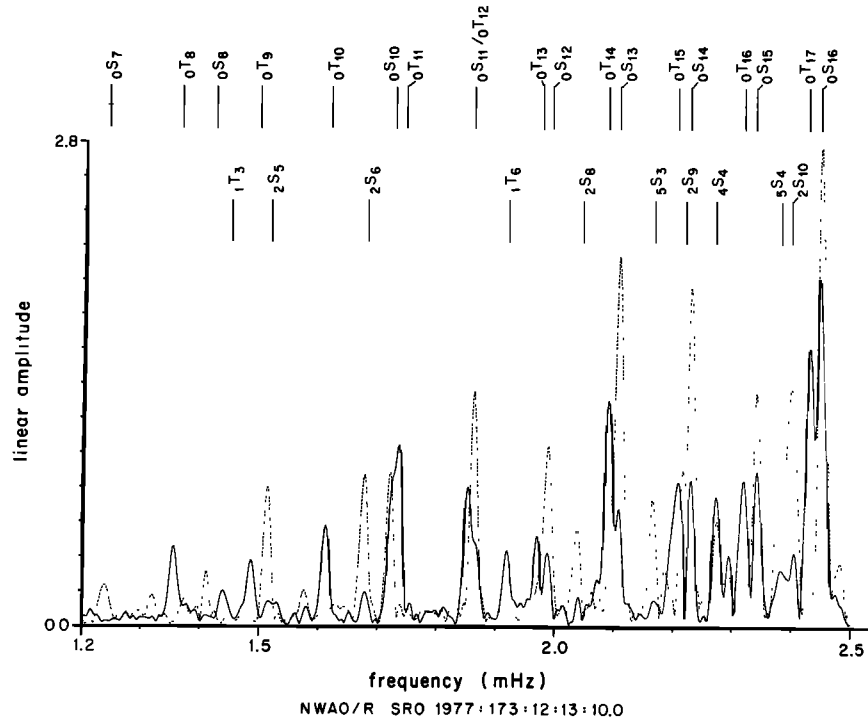
Fig. 15. Spectra of 40-hour Hanning-tapered records for NWAO/Tonga 1977. Radial (dashed line) and transverse (solid line) spectra showing $_0S_l - _0T_{l+1}$ coupling.

or $_0S_l - _0T_{l-1}$. It seems that proximity in angular order, l, as well as in complex frequency is required to produce observable coupling. Also the type of mode, S or T, is important. For example $_0T_7$ and $_0S_7$ differ in frequency by only 8.8 μHz and have Q values of about 200 and 400, respectively, but are not observed to be coupled. These factors suggest that we are correct in identifying Coriolis

coupling as the dominant factor rather than anisotropy or aspherical structure.

In our experiments, aspherical structure does cause noticeable changes in the calculated spectra of very strongly coupled modes. In principle, we could use this feature to distinguish between competing models of aspherical structure. In practice, such an experiment
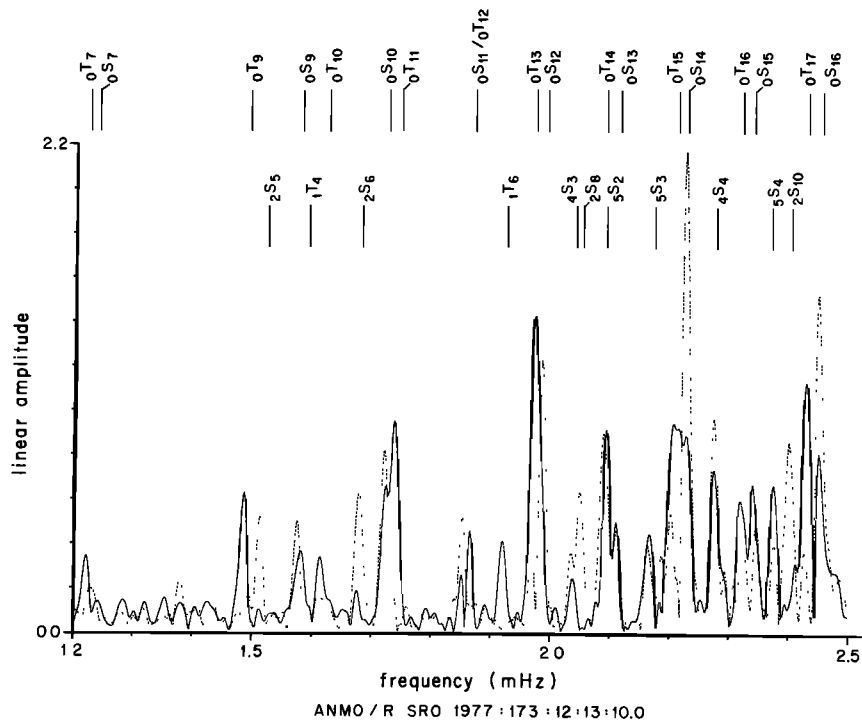

Fig. 16. As in Figure 15 for ANMO/Tonga 1977. Several St modes appear on the transverse component.

TABLE A1.   A Simple Q Model with Bulk Q Constrained to be at Least $50 \times$ Shear Q

| Shell Radii, km | Model Parameters | |
	Shear Q	Bulk Q
0—1229	3140	157,000
3484—5700	332	16,600
5700—5950	277	13,850
5950—6371	118	5,895

would be premature. A very precise model of the spherically averaged structure is required because the very strong coupling is sensitive to the exact relative locations of the fundamental spheroidal and toroidal mode branches. Such a model is not yet available.

The differences between the computed spectra for a spherical earth and for more realistic (though very simple) models demonstrate the potential for bias in source mechanism retrieval if coupling is ignored. It may be possible to misinterpret the coupling signal as a complex source mechanism. We are currently investigating this matter, and we suspect that coupling may explain some of the difficulties we have experienced in retrieving source mechanisms, particularly those of shallow events.

A reexamination of the methods used to infer aspherical structure is also required in the frequency bands where

coupling is strong. The shifts in peak frequency reported by *Silver and Jordan* [1981] and *Masters et al.* [1982] represent observations of singletlike multiplet peaks. These peak shifts exhibit a clear dependence on source-receiver path and led to a preliminary inversion for aspherical structure using the asymptotic theory for uncoupled modes derived by *Jordan* [1978]. The mean peak shift of an uncoupled mode when averaged over all source-receiver orientations would be zero, a consequence of the diagonal sum rule. This is not true for coupled hybrid modes as demonstrated in Figure 6. At frequencies below about 3.0 mHz we observe St modes, and we would expect the peak shifts of these modes to show a different dependence on source-receiver location from uncoupled spheroidal modes. This feature can be seen in Figure 2 of *Masters et al.* [1982], where the spherical harmonic coefficients of the peak shift patterns are clearly perturbed by the coupling effects for $_0St_8 - _0St_{20}$. It is obviously desirable to extend the theory for interpreting peak shifts to include the coupled hybrid modes.

In summary, the frequency repulsion, attenuation averaging, and amplitude variation in the hybrid multiplets are observed features that must be taken into account in studies of models of density, elastic structure, and anelastic structure and in studies of earthquake source mechanisms. The computational problem at low frequencies is

TABLE A2.   Fundamental Spheroidal Mode Frequency and Attenuation Values

Degree	Frequency, mHz	Standard Deviation, μHz	$1000/Q$	Standard Deviation	No. of Observations[*]
8	1.41240	0.15	2.72	0.10	118
9	1.57675	0.15	2.91	0.07	186
10	1.72363	0.15	3.00	0.08	188
11	1.86280	0.30	4.14	0.18	63
12	1.99093	0.15	3.18	0.06	172
13	2.11320	0.15	3.23	0.03	261
14	2.23109	0.15	3.30	0.05	202
15	2.34620	0.20	3.14	0.04	246
16	2.45833	0.15	3.40	0.04	261
17	2.56722	0.15	3.74	0.05	219
18	2.67330	0.30	4.10	0.05	236
19	2.77602	0.35	4.37	0.06	257
20	2.87670	0.35	3.93	0.06	237
21	2.97614	0.15	3.84	0.04	361
22	3.07388	0.15	3.93	0.04	331
23	3.17032	0.15	4.00	0.03	446
24	3.26520	0.25	4.09	0.06	278
25	3.35880	0.15	4.29	0.05	300
26	3.45135	0.20	4.30	0.05	345
27	3.54305	0.20	4.53	0.05	328
28	3.63425	0.25	4.73	0.05	350
29	3.72440	0.15	4.62	0.05	390
30	3.81464	0.25	4.76	0.07	274
31	3.90480	0.30	5.12	0.08	262
32	3.99416	0.25	5.15	0.08	239
33	4.08296	0.20	5.48	0.06	337
34	4.17130	0.30	5.25	0.09	216
35	4.26125	0.35	5.61	0.11	153
36	4.35090	0.30	5.56	0.07	209
37	4.44050	0.40	5.57	0.07	194
38	4.52984	0.30	5.77	0.06	213
39	4.61830	0.50	6.03	0.13	108
40	4.70740	0.40	6.10	0.14	111
41	4.79795	0.60	6.23	0.12	98
42	4.88795	0.75	6.27	0.18	56
43	4.97702	0.30	6.32	0.15	57

[*]Total number of observations is 8302.

made more complicated by multiplet coupling but leads to a more refined analysis of the complex frequency data and complex amplitude data.

That strong coupling is very sensitive to structure is a severity that must be overcome in the analysis. In the long run it may prove to be a blessing in disguise because the details of strong coupling, if they can be observed, should provide very strong constraints on some features of models of the earth.

APPENDIX

The model of attenuation used in this paper has been derived from 57 observed mean attenuation data. The data have been adjusted to remove the effect of coupling. Let $q = Q^{-1}$ and define

q_M calculated value of q with no coupling;

q_C calculated value of q in the presence of rotation, ellipticity of figure and aspherical structure;

q_O observed value of q;

q_A adjusted observation with coupling effects removed.

Then, for a good model of attenuation, by definition $q_O - q_C = q_A - q_M$ or

$$q_A = q_O - (q_C - q_M) \qquad (A1)$$

We have applied (A1) to the observations of $_0S_\ell$ for $\ell = 8\text{--}46$. Both q_C and q_M were calculated from the model in Table 9 of *Masters and Gilbert* [1983]. The remaining data were not adjusted for coupling effects. The $_0S_\ell$ data of *Masters and Gilbert* [1983], derived from 557 IDA records, have been supplemented. The new $_0S_\ell$ dataset has been derived from 950 IDA records and 250 GDSN vertical records.

Using the adjusted dataset, we have derived the model listed in Table A1. The details of the inversion procedure are given by *Masters and Gilbert* [1983]. We regard the model in Table A1 to be an interim model, derived primarily to provide a better fit to the observed data with coupling effects modelled according to (A1). Eventually, we should be able to model the observed attenuation of individual singlets, and the expedient of using (A1) can be surpassed. The new $_0S_\ell$ dataset is given in Table A2.

REFERENCES

Akopyan, S. T., V. N. Zharkov, and V. M. Lyubimov, The dynamic shear modulus in the interior of the earth, *Dokl. Acad. Sci. USSR Earth Sci. Sect., 223,* 1–3, 1975.

Akopyan, S. T., V. N. Zharkov, and V. M. Lyubimov, Corrections to the eigenfrequencies of the earth due to the dynamic shear modulus, *Izv. Acad. Sci. USSR Phys. Solid Earth, 12,* 625–630, 1976.

Backus, G. E., and J. F. Gilbert, The rotational splitting of the free oscillations of the earth, *Proc. Natl. Acad. Sci. 47,* 362–371, 1961.

Baker, C. T. H., *The Numerical Treatment of Integral Equations,* Clarendon, Oxford, 1977.

Benioff, H., F. Press, and S. W. Smith, Excitation of the free oscillations of the earth by earthquakes, *J. Geophys. Res., 66,* 605–619, 1961.

Dahlen, F. A., The normal modes of a rotating, elliptical Earth, *Geophys. J. R. Astron. Soc., 16,* 329–367, 1968.

Dahlen, F. A., The normal modes of a rotating, elliptical earth, II, Near resonance multiplet coupling, *Geophys. J. R. Astron. Soc., 18,* 397–436, 1969.

Dahlen, F. A., The effect of data windows on the estimation of free oscillation parameters, *Geophys. J. R. Astron. Soc., 69,* 537–549, 1982.

Dahlen, F. A., and R. V. Sailor, Rotational and elliptical splitting of the free oscillations of the earth, *Geophys. J. R. Astron. Soc., 58,* 609–623, 1979.

Dziewonski, A., and D. Anderson, Preliminary reference earth model, *Phys. Earth Planet. Inter., 25,* 297–356, 1981.

Finlayson, B. A., *The Method of Weighted Residuals and Variational Principles,* Academic, New York, 1972.

Garbow, B., J. Boyle, J. Dongarra, and C. Moler, *Matrix Eigensystem Routines—EISPACK Guide Extension,* Lecture Notes in Computer Science, Springer-Verlag, New York, 1977.

Gilbert, F., The diagonal sum rule and averaged eigenfrequencies, *Geophys. J. R. Astron. Soc., 23,* 125–128, 1971.

Gilbert, F., and A. Dziewonski, An application of normal mode theory to the retrieval of structural parameters and source mechanisms from seismic spectra, *Philos. Trans. R. Soc. London Ser. A, 278,* 187–269, 1975.

Jordan, T. H., A procedure for estimating lateral variations from low-frequency eigenspectra data, *Geophys. J. R. Astron. Soc., 52,* 441–455, 1978.

Kanamori, H, and D. L. Anderson, Importance of physical dispersion in surface wave and free oscillations problems: review, *Rev. Geophys. Space Phys., 15,* 105–112, 1977.

Kantorovich, L. V. and V. I. Krylov, *Approximate Methods of Higher Analysis,* P. Noordhoff, Groningen, 1958.

Kawakatsu, H., and R. J. Geller, A new iterative method for finding the normal modes of a laterally heterogeneous body, *Geophys. Res. Lett., 8,* 1195–1197, 1981.

Liu, H.-P., D. L. Anderson, and H. Kanamori, Velocity dispersion due to anelasticity; implications for seismology and mantle composition, *Geophys. J. R. Astron. Soc., 47,* 41–58, 1976.

Luh, P. C., Free oscillations of the laterally inhomogeneous Earth: Quasi degenerate multiplet coupling, *Geophys. J. R. Astron. Soc., 32,* 187–202, 1973.

Luh, P. C., The normal modes of the rotating self gravitating inhomogeneous earth, *Geophys. J. R. Astron. Soc., 38,* 187–224, 1974.

MacDonald, G. J. F., and N. F. Ness, A study of the free oscillations of the earth, *J. Geophys. Res., 66,* 1865–1911, 1961.

Madariaga, R. I., Free oscillations of the laterally heterogeneous earth, Ph.D. thesis, 105 pp., Mass. Inst. of Technol., Cambridge, 1971.

Marchuk, G. I., *Methods of Numerical Mathematics,* Springer-Verlag, New York, 1975.

Masters, G., and F. Gilbert, Attenuation in the earth at low frequencies, *Philos. Trans. R. Soc. London Ser. A, 308,* 479–522, 1983.

Masters, G., T. H. Jordan, P. G. Silver, and F. Gilbert, Aspherical earth structure from fundamental spheroidal-mode data, *Nature, 298,* 609–613, 1982.

Mikhlin, S. G., *Variational Methods in Mathematical Physics,* MacMillan, New York, 1964.

Moiseiwitsch, B. L., *Variational Principles,* John Wiley, New York, 1966.

Morris, S. P., and R. J. Geller, Toroidal modes of a simple laterally heterogeneous sphere, *Bull. Seismol. Soc. Am., 72,* 1155–1166, 1982.

Ness, N. F., C. J. Harrison, and L. J. Slichter, Observations of the free oscillations of the earth, *J. Geophys. Res., 66,* 621–629, 1961.

Pekeris, C. L., A. Alterman, and M. Jarosch, Rotational multiplets in the spectrum of the earth, *Phys. Rev., 122,* 1692–1700, 1961.

Riedesel, M., T. H. Jordan, and G. Masters, Observed effects of lateral heterogeneity on fundamental spheroidal modes (abstract), *Trans. AGU Eos, 62,* 332, 1981.

Silver, P. G., and T. H. Jordan, Fundamental spheroidal mode observations of aspherical heterogeneity, *Geophys. J. R. Astron. Soc., 64*, 605–634, 1981.

Smith, B., J. Boyle, J. Dongarra, B. Garbow, Y. Ikebe, V. Klema, and C. Moler, *Matrix Eigensystem Routines—EISPACK Guide*, Lecture Notes in Computer Science, Springer-Verlag, New York, 1976.

Smith, M. L., Wobble and rotation of the earth, *Geophys. J. R. Astron. Soc., 50*, 103–140, 1977.

Smith, M. L., and F. A. Dahlen, The period and Q of the Chandler wobble, *Geophys. J. R. Astron. Soc., 64*, 223–281, 1981.

Sommerfeld, A., *Mechanics, Lectures on Physics*, vol. 1, 289 pp., Academic, New York, 1952.

Woodhouse, J. H., On Rayleigh's principle, *Geophys. J. R. Astron. Soc., 46*, 11–22, 1976.

Woodhouse, J. H., The coupling and attenuation of nearly resonant multiplets in the earth's free oscillation spectrum, *Geo-phys. J. R. Astron. Soc., 61*, 261–283, 1980.

Woodhouse, J. H., and F. A. Dahlen, The effect of a general aspherical perturbation on the free oscillations of the earth, *Geophys. J. R. Astron. Soc., 53*, 335–354, 1978.

Zharkov, B. N., and V. M. Lyubimov, Torsional oscillations of a spherically asymmetrical model of the earth, *Izv. Acad. Sci. USSR Phys. Solid Earth, no. 2*, 71–76, 1970a.

Zharkov, B. N., and V. M. Lyubimov, Theory of spheroidal vibrations for a spherically asymmetrical model of the earth, *Izv. Acad. Sci. USSR Phys. Solid Earth, no. 10*, 613–618, 1970b.

F. Gilbert, G. Masters, and J. Park, Institute of Geophysics and Planetary Physics, A-025, Scripps Institution of Oceanography, La Jolla, CA 92093.